Journal of Energy

VOLUME 67 Number 1 | 2018 Special Issue

journal homepage: http://journalofenergy.com/

Martin Dadić
University of Zagreb
Faculty of Electrical Engineering and Computing / FER
Zagreb, Croatia, martin.dadic@fer.hr

Tomislav Župan
KONČAR - Electrical Engineering Institute, Inc
Transformer Department, R&D Section
Zagreb, Croatia, tzupan@koncar-institut.hr

Gabrijel Kolar
University of Zagreb
Faculty of Electrical Engineering and Computing / FER
Zagreb, Croatia, gabrijel.kolar@fer.hr

Finite-Impulse-Response Modeling of Voltage Instrument Transformers Applicable for Fast Front Transients Simulations

Summary

This paper presents a method for Finite-Impulse-Response (FIR) modeling of voltage instrument transformers. The method is based on Wiener filtering and measurement of the transformer response in the frequency domain using a low frequency network analyzer. The proposed method allows, through digital filtering operation, an accurate simulation of the transformer response to transient excitation. Furthermore, the proposed approach to the modeling of the system function allows unequal spacing of the frequency samples. The linearity of the transformer is analyzed applying the Fourier analysis and different waveforms of the primary voltage, and methods for the model order selection, based on the generalized information criterion, are discussed and applied. The theoretical analysis is confirmed with measurements in time domain, using the recurrent surge generator.

Key words: transformer model, black-box, Wiener filetring, FIR filters, transfer function measurement, recurrent surge generator, lightning impulse

Introduction

Since transformers are typically constructed to work almost continuously during a period of forty years or more, they should be able to withstand both steady-state operation as well as possible transients in power grid. Most of the time the transformers are subjected to variations of less than 10% nominal voltage and 1% nominal frequency. All other types of excitation are considered as transients. Some of the typical causes of transients within the power grid are short circuits, switching operations, atmospheric discharges and almost any other changes within the system. Stresses that the insulation has to withstand can often have a great impact on design, performance and the overall price of the equipment. Standards typically classify transients into four groups (IEC 60071-2, 1996; IEEE 1313.2, 1999): low-frequency transients, slow front transients, fast front transients and very fast front transients. This paper focuses on the fast front transients which are normally aperiodic waves associated with near atmospheric discharges with a front time between 0.1 and 20 μs.

Due to various switching operations and atmospheric discharges, transformers are exposed to numerous overvoltages and have to be designed to correctly operate in those circumstances. The effects of transients are primarily visible on the transformer windings. The winding's ability to withstand overvoltages is determined by the shape of the transient signal, winding's geometry, characteristics of the insulation material and the overall condition of the winding including its age and past exposition to transients. A great number of transformer faults occur due to the insulation breakdown between turns of the winding. Steady state voltages under nominal grid frequency distribute linearly across the turns of the transformer winding and can be precisely determined. However, fast front transients usually lead to highly nonlinear voltage distribution. This often leads to high voltage stresses, especially at the beginning sections of the winding. Therefore, adequate mathematical models are needed to study the winding behavior at voltages with high frequency components.

Two main approaches to the transient modeling of transformers can be found in the literature published until today: the first one tries to accurately model the internal winding structure of transformers by modeling the capacitances, self- and mutual inductances and resistances. The second approach uses a black-box approach, where a model is built solely on the input/output data acquired during properly chosen experiments. In [1] the black box-approach uses bilinear transformation to build a discrete-time, z-domain model. In [2] a system identification approach is applied in a pole-zero sub-space modeling of distribution transformers intended primarily for the transformer fault-detection. This was done using frequency response analysis (FRA) measurements. In [3] a review of the applications of *z*-transform in electromagnetic transient simulations of power systems is given, with presented applications in transmission line modeling and power networks. In [4] a detailed overview of frequency-domain measurements methods for the validation of transformer models is given, alongside with methods for their rational-function approximation and re-

cursive convolution procedures for obtaining time-domain responses. In [5] a method for the black-box estimation of power transformers using the measurements performed with commercially available frequency-response-analyzers is presented. Since FRA equipment, dedicated for transformer measurements, measure input and output voltages grounded through matching resistors, a method based on two-independent measurements was developed that finally gives the admittance matrix, which can be used for the conversion to time-domain for no-load condition.

The main purpose of this paper is to provide a measurement procedure and a tool for the black-box estimation of conveying the fast or lightning transients of the voltage instrument transformers.

The approach is based on the frequency-domain measurements, and the measured response is used to build a discrete-time, Finite Impulse Response (FIR) transformer model. Once determined, FIR model allows, through the digital filtering operation, a very easy time-domain calculation of the system's response at any transient excitation. Through the digital filtering operation (closely related to the concept of recursive convolution [1]), the model output at any sample number n can be calculated by summation:

$$y(n) = w_0 x(n) + w_1 x(n-1) + ... + w_L x(n-L) \quad (1)$$

where L denotes model order, $x(n)$ is time-sampled input signal, and w_l are FIR model coefficients.

Wiener Filtering

Let a real input sequence x_k and a desired real output sequence d_k for k=0,1,2,… be given. The goal of Wiener filtering [6] is to find an Lth-order FIR filter (with filter coefficients w_0,….w_L)

$$H(z) = \sum_{r=0}^{L} w_r z^{-r} \quad , \quad (2)$$

which produces from the input, x_k, an estimate, d'_k , that minimizes the error between desired and modeled response.

This is a reduced-order approximation of the true impulse response of the system $H(\times)$. Here, w_r are filter coefficients, and z denotes the variable in the z-domain.

Its frequency response is characterized by

$$H(f) = \sum_{k=0}^{L} w_k e^{-jk2\pi fT} \quad 3)$$

where T denotes sample interval and f is the frequency.

The optimal solution of filter coefficients is obtained by solving the time-discrete Wiener-Hopf equation [6] .

$$\mathbf{Rw} = \mathbf{p} . \quad (4)$$

Here **R** denotes the autocorrelation matrix of the input, x_k

$$\mathbf{R} = \begin{bmatrix} r_{xx}(0) & r_{xx}(1) & ..... & r_{xx}(L) \\ r_{xx}(1) & r_{xx}(0) & ..... & r_{xx}(L\text{-}1) \\ . & & & \\ . & & & \\ r_{xx}(L) & r_{xx}(L\text{-}1) & & ..... \; r_{xx}(0) \end{bmatrix} \quad (5)$$

R is a symmetric Toeplitz matrix. The cross-correlation vector, **p**, between the desired response, d_k, and the input, x_k, reads as follows [6]:

$$\mathbf{p} = \begin{bmatrix} r_{dx}(0) & r_{dx}(1) & ..... & r_{dx}(L) \end{bmatrix}^{\mathrm{T}} \quad (6)$$

Further,

$$\mathbf{w} = \begin{bmatrix} w_0 & w_1 & ..... & w_L \end{bmatrix}^{\mathrm{T}} \quad (7)$$

denotes the coefficient vector of the Lth-order Wiener filter.

The Wiener-Hopf equation will not have a unique solution unless the equations are independent.

The transfer function to be modeled can be described in the frequency domain by a set of complex frequency samples:

$$H(\phi_l) = a_l \exp(j\theta_l) \quad , \quad l = [1, N]. \quad (8)$$

Here, defines magnitude response, defines phase response, and is the set of discrete frequencies for which the transfer function is defined. According to the Shannon sampling theorem, the sampling frequency f_s=1/T should be greater than twice the maximum frequency . Here, T denotes the sample interval.

For the system described by the transfer function (3), the input autocorrelation matrix, **R**, and the desired-to-input cross-correlation vector, **p**, are finally [7]:

$$\mathbf{R} = \frac{1}{2} \begin{bmatrix} \sum_{l=1}^{N} c_l^2 & \sum_{l=1}^{N} c_l^2 \cos 2\pi\phi_l T & ..... & \sum_{l=1}^{N} c_l^2 \cos 2L\pi\phi_l T \\ \sum_{l=1}^{N} c_l^2 \cos 2\pi\phi_l T & \sum_{l=1}^{N} c_l^2 & & \\ . & & & \\ . & & & \\ \sum_{l=1}^{N} c_l^2 \cos 2L\pi\phi_l T & . ..... & ..... & \sum_{l=1}^{N} c_l^2 \end{bmatrix} \quad (9)$$

$$\mathbf{p} = \frac{1}{2} \begin{bmatrix} \sum_{l=1}^{N} a_l c_l^2 \cos(\theta_l) \\ \sum_{l=1}^{N} a_l c_l^2 \cos(2\pi\phi_l T + \theta_l) \\ . \\ . \\ \sum_{l=1}^{N} a_l c_l^2 \cos(2L\pi\phi_l T + \theta_l) \end{bmatrix} \quad (10)$$

Here, denotes the sample interval, i.e. distance between samples, and c_l is a frequency-dependent positive weighting factor.

A Wiener-Hopf equation describes a system of linear equations that has a unique solution if **R** is a nonsingular matrix, i.e. if it is invertible [8]. In such a case, the system can generally be solved using Gaussian elimination. For some nonsingular matrices, the solution can also be found using certain factorization methods or iterative methods [9]. The Toeplitz structure of **R** allows application of Levinson's or Trench's algorithm as well [10].

A Wiener–Hopf equation (4) describes a system of linear equations that has a unique solution if **R** is a nonsingular matrix. Since every positive definite matrix is nonsingular [8], if the autocorrelation matrix is positive definite, it would be invertible. The matrix R is guaranteed to be a positive definite if the input signal $x(t)$ is spectrally rich, which will be fulfilled if there is at least half as many frequency components in $x(t)$ as there are coefficients in the Wiener filter [11], [12]. This condition will be easily satisfied with the increased number of the frequency samples in the measurements. In such a case, the solution of the system of equations (4) can be easily found using the MATLAB function *mldivide*, which performs Gaussian elimination for $n \times n$ square matrices and column vectors with n components. This technique was applied in all cases presented in the subsequent sections.

It was observed in our measurements, that measured transfer function, once converted from the frequency into time domain, may tend to be shifted "in advance". This does not cause any problem when dealing with the Fourier series, due to its time-periodicity. In system identification, it makes the impulse response of the target system noncausal. To include this shifted, "negative-time" portion of the system's impulse response in the model, it is wise to introduce a time delay in the desired response d_k for a fixed number of samples. In the frequency domain, it is performed by multiplication of the complex transfer function with , where n_0 denotes the delay in samples, T is sample interval and f is frequency. The possible causes of this phenomenon can be attributed to imperfections in the "through" calibration or measurement errors. It was also observed in radio-frequency measurements [13] and in FEM simulations [14] with the same solution. The modeling delay is discussed in more details in [15].

Measurement Set-Up

The measurements for the frequency-domain modeling of transformers can be divided in two approaches [4]:

— *voltage transfer measurements*
— *admittance matrix measurements*

For linear-time-invariant systems, the second approach gives a possibility of calculating the response for different loads (including no-load condition), while the voltage transfer measurement gives the response for the no-load condition or for a fixed load. Regarding the linearity, the model is assumed to be linear [5] since its experimental verification was carried out at low voltage in comparison to nominal voltages. This is generally the case for routine lightning-impulse testing of transformers.

The modeling procedure proposed in this paper applies the voltage transfer measurement, which was performed using a LF-RF network analyzer Keysight ENA 5061B and gain-phase test port. The LF option enables measurement of voltage transfer functions for frequencies spanning from 5 Hz to 30 MHz using the gain-phase port, while the input impedance can be switched between 50 Ω and 1 MΩ. The possibility of setting the high input impedance (1 MΩ) allows using high impedance oscilloscope probes with ratio 10:1 and 10 MΩ input impedance (shunted with the probe capacitance), which is approximately the same load applied with the oscilloscope probe in the time-domain measurements with the recurrent surge generator. Therefore, two oscilloscope probes Agilent 2862A (15 pF, 10 MΩ) were used in the measurement, and the "through" calibration of the analyzer was performed prior to measurements, which eliminates the influence of the probes on the measurement. This is especially important for the measurements in the MHz range. Use of high impedance (10 MΩ) probes further enhances the measurement in the MHz range, since using a 10:1 passive probes for oscilloscopes generally gives small input capacitance around 10 pF at the probe end. In this way, the load impedance is significantly increased when comparing to 1:1 passive probes. Similarly to general oscilloscope applications, it is an orthodox way for high impedance probing at higher frequencies [16]. The measurements were performed in the frequency range 5 Hz to 3 MHz, with the intermediate frequency bandwidth (IFBW) equal to 2 Hz. Use of low values of IFBW improves the measurement results, and in the same time slows the measurement process. For the same frequency range, increasing the IFBW to 100 Hz makes the measurement significantly faster, and does not the corrupt the results. The time-domain measurements were performed using a recurrent surge generator Haefely 481 and digital oscilloscope Tektronix DPO4054 equipped with voltage probes Tektronix P6139A (8 pF, 10MΩ). The FIR modeling was performed using a custom-made program in MATLAB, with sampling frequency equal to 6.004 MHz, which ensures, due to the Shannon sampling theorem the upper frequency limit of 3 MHz. To avoid non-causal response, a fixed modeling delay of 5 samples is introduced in measured transfer function.

The transformer is a voltage instrument transformer designed and manufactured in our laboratory for a digital sampling wattmeter application [17]. Its characteristics are as follows: nominal primary voltage is 230 V (RMS) at 50 Hz, class 1 according to IEC 61869-3, the targeted number of turns in the primary winding was N_p=1336 and N_s=45 in the secondary winding. The targeted maximum flux density at the primary voltage of 250 V (RMS) was set to 0.6 T, which ensures that the magnetic flux density is far bellow the saturation knee even at the primary voltage equal to 120% of its nominal value. The wire diameter in the secondary was chosen to be big enough to allow the secondary winding to be wound in a complete layer. Due to the high turn ratio, it was possible only with relatively big wire diameters, and the wire diameter of the secondary was chosen to be 1.2 mm. The wire diameter of the primary is 0.22 mm. In this way, each of the two sections of the primary consists of 4 complete layers. All layers were mutually isolated using the cellulose paper to allow easier assembling. The final number of turns was slightly different of the targeted, because all layers were wound completely to the edge of the former. The transformer core was a standard CM core CM85 (CM85b, older label SM85) core produced by Iskra Sistemi d.d. The CM cores consist of four core halves, with the coil former on the middle leg. To decrease leakage inductances and distributed capacitances, the sectionalized primary winding [18]-[21] with simple interleave was applied (Fig. 1). Due to the small burden (input impedance of the acquisition card NI-4461), the rated output of the VIT was chosen to be 1 VA at power factor 1. Fig. 2 presents the photo of the transformer.

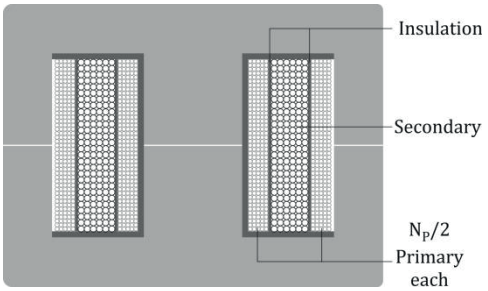

Figure 1. Configuration with simple interleave – sectionalized primary

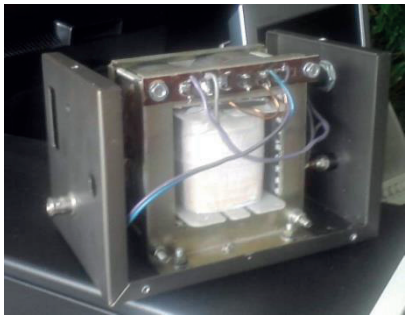

Figure 2. Transformer with the opened housing

Non-linearity analysis

Table I . Harmonic components of the secondary voltage for the single-tone stimulus

Harmonic order	1	2	3	4	5	6	7	8	9	10
Frequency (Hz)	50	100	150	200	250	300	350	400	450	500
Magnitude (%, compared to the fundamental)	100	0	0.8	0.7	0.3	0.1	0.4	0.1	0.1	0.2

The assumed linearity of the target system between primary and secondary voltages was further investigated applying the single-tone and multi-tone excitation and Fourier analysis. The nonlinear transfer function of a system generates the higher harmonic components at the output of the system, when the pure sine stimulus is applied. For the multi-tone excitation, the intermodulation occurs as well. The targeted maximum flux density in the transformer core, at the primary voltage of 250 V (RMS) was set in the design to 0.6 T, which ensures that the magnetic flux density is far below the saturation knee even at the primary voltage equal to 120% of its nominal value. Thus, for the nominal primary voltage and primary voltages lower than the nominal, it is expected that the relationship between primary and secondary voltage is nearly linear in the no-load condition. The measurement set-up for the non-linearity analysis was consisted of a Calmet C300 three phase power calibrator and tester and the power analyzer Chauvin-Arnoux CA8220. The sinusoidal distortion of the primary voltage, as declared by the calibrator manufacturer (Calmet) is 0.05 %.

In the first set of the measurements, the single-tone voltage was applied at the primary, where the primary voltage was nominal (e.g. 230 V, 50 Hz). At the secondary the RMS values of the first 10 harmonics were measured, as well as the total harmonic distortion in relation to the fundamental (THD_F) for the first 50 harmonic components. THD_F is expressed as

$$\mathrm{THD_F} = \frac{\sqrt{I_2^2 + I_3^2 + \ldots\ldots + I_n^2}}{I_1}, \tag{11}$$

where I_1 denotes magnitude of the fundamental harmonic, and I_2 to I_n denote magnitudes of the higher harmonics. The measured THD_F of the secondary voltage was 1.5 %, while the RMS values of the first 10 harmonic components, in percentages compared to the fundamental are systemized in the Table I.

For the two-tone excitation, the further insight in the generation of the intermodulation components can be obtained using the following analysis: Suppose that the non-linear transcharacteristic of the system can be

expanded about the operating point by mean of power series

$$e_o = a_0 + a_1 e_i + a_2 e_i^2 + a_3 e_i^3 \tag{12}$$

where e_i and e_o are the alternating parts of the input and output voltages. If the input signal is composed of two cosines with radian frequencies p and q,

$$e_i = P\cos(pt) + Q\cos(qt) \tag{13}$$(13)

the harmonic distortion and intermodulation components are [22]:

$$\begin{aligned} e_o = &\left(\frac{1}{2}a_2P^2 + \frac{1}{2}a_2Q^2\right) + \left(a_1P + \frac{3}{4}a_3P^3 + \frac{3}{2}a_3PQ^2\right)\cos(pt) \\ &+ \left(a_1Q + \frac{3}{4}a_3Q^3 + \frac{3}{2}a_3P^2Q\right)\cos(qt) \\ &+ \frac{1}{2}a_2P^2\cos(2pt) + \frac{1}{2}a_2Q^2\cos(2qt) \\ &+ \frac{1}{4}a_3P^3\cos(3pt) + \frac{1}{4}a_3Q^3\cos(3qt) \\ &+ a_2PQ[\cos(p+q)t + \cos(p-q)t] \\ &+ \frac{3}{4}a_3P^2Q[\cos(2p+q)t + \cos(2p-q)t] \end{aligned} \tag{14}$$

More generally, if the input signal is consisted of the two sine components, it is expected that the non-linear transfer function (transcharacteristic) generates both the higher harmonic components of each input sine (with the radian frequencies 2p, 3p ,,, 2q, 3q, etc.) and the intermodulation components with the radian frequencies p+q , p-q , 2p+q , 2p-q , etc. For the input voltage consisted of two sine tones with the frequencies equal to 50 and 100 Hz, it is this expected that at the output of the system the second-order summation component with the frequency equal to 150 Hz is certainly present.

Figure 3. Two-tone waveform

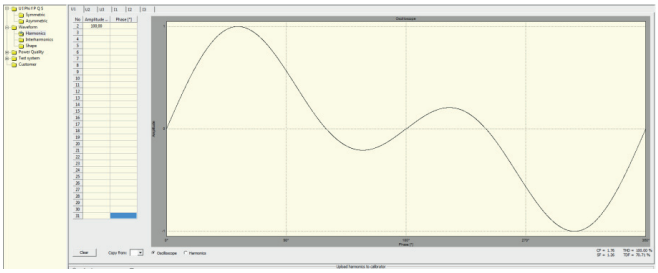

In the second set of measurements, the primary voltage generated by the calibrator was consisted of two sine tones with the equal magnitudes and frequencies 50 Hz and 100 Hz. Fig. 3 presents the waveform of the primary voltage. The RMS value of this composite voltage was set again to 230 V RMS. In the Table II, the harmonic analysis of the secondary voltage is presented.

Table II . Harmonic components of the secondary voltage for the two-tone stimulus

Harmonic order	1	2	3	4	5	6	7	8	9	10
Frequency (Hz)	50	100	150	200	250	300	350	400	450	500
Magnitude (%, compared to the fundamental)	100	99.5	0.7	0.8	0.4	0.2	0.4	0.4	0.4	0.4

It can be seen from the Tables I and II, that the magnitudes of the generated higher harmonic components are negligible, compared to the fundamental and that the THD_F is low at the secondary for a single-tone excitation. Moreover, for the two-tone excitation, the magnitude of the summation tone (150 Hz) is equal to its relative magnitude for the single-tone excitation, which further approves that the intermodulation components are negligible, and that the system can be regarded as linear. It should be pointed that the whole analysis is presented for the primary and secondary voltages, which are the measured parameters for both FRA and impulse response analysis. The possibly non-sinusoidal magnetization current therefore does not influence the assumed linearity of the relationship between the primary and secondary voltages.

Results

Standard lightning impulse (LI)

The first set of time-domain measurements was performed with the standard lightning impulse (1,2 μs/50 μs) according to IEC 60060-1. The sample interval of the oscilloscope in the time-domain measurements with the recurrent surge generator was 10 ns. To match the exciting signal with the sample period of the FIR model (e.g. = 0.16656 μs), the LI was resampled using MATLAB function *interp*. The filter order was L=300 (i.e. the overall number of the coefficients was 301), and the modeling delay was 5 samples. The frequency-dependent positive weighting factors c_l were all set to 1. Fig. 4 presents the frequency response (magnitude) of the model, compared to the frequency domain measurements using the network analyzer. Fig. 5 depicts the measured input voltage, while Fig. 6 presents the simulated response. The simulated response is the result of the digital filtering operation using the estimated FIR model and measured excitation. Fig. 7 gives the comparison of the simulated and measured response in the time-domain. The simulated time-domain response is shifted “in left” for 5 samples, to compensate the modeling delay.

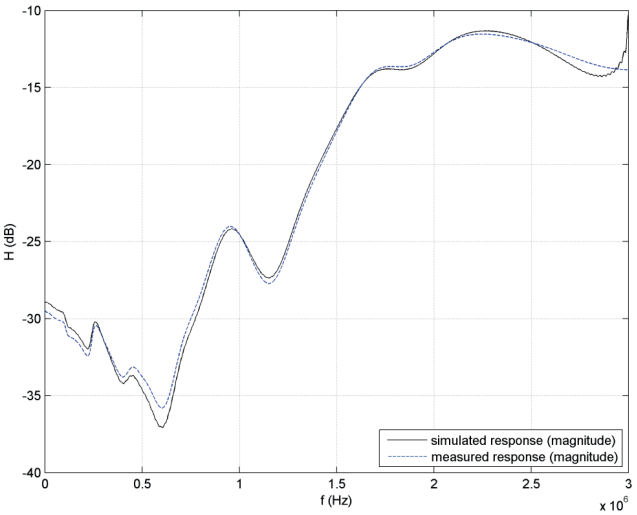

Figure 4. Comparison of measured and modeled transfer function - magnitude

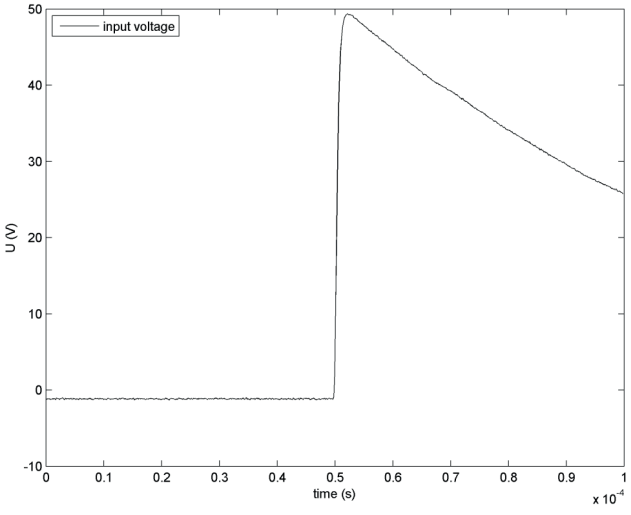

Figure 5. Measured excitation – full wave

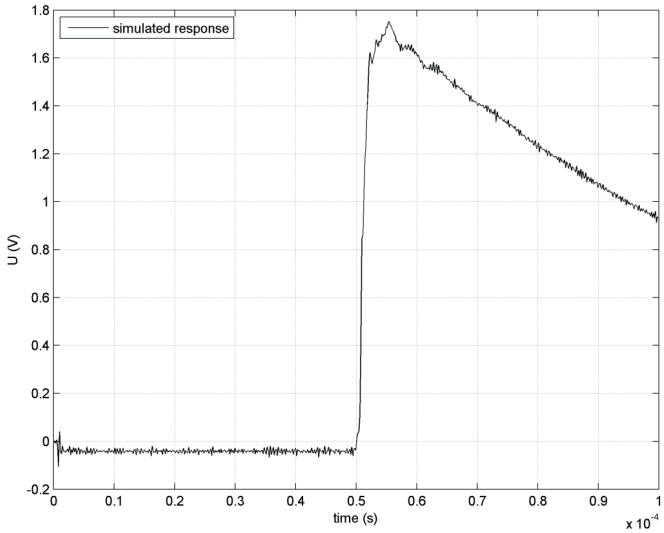

Figure 6. Simulated response – full wave

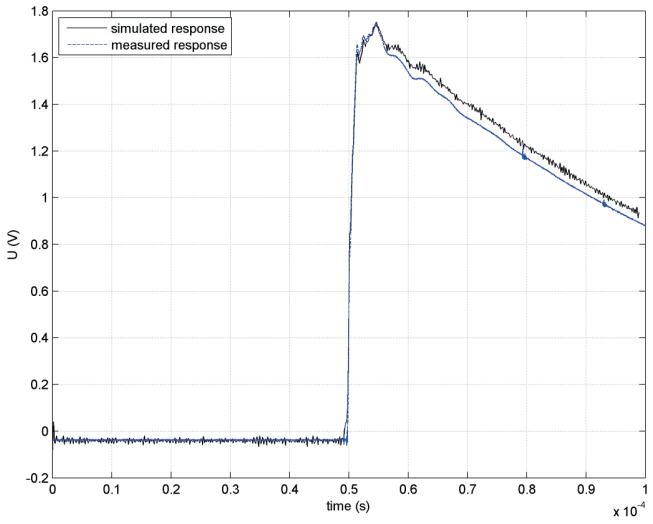

Figure 7. Comparison of measured and simulated response for the full wave excitation

Lightning impulse chopped on the front (LI-CF)

The second set of time-domain measurements was performed using the lightning impulse chopped on the front according to IEC 60060-1. All settings were the same as in (A), except the sample interval of the oscilloscope, which was 4 ns. Fig. 8 depicts the measured input voltage, while Fig. 9 gives the comparison of the simulated and measured response in the time-domain. The simulated time-domain response is shifted “in left” for 5 samples, to compensate the modeling delay.

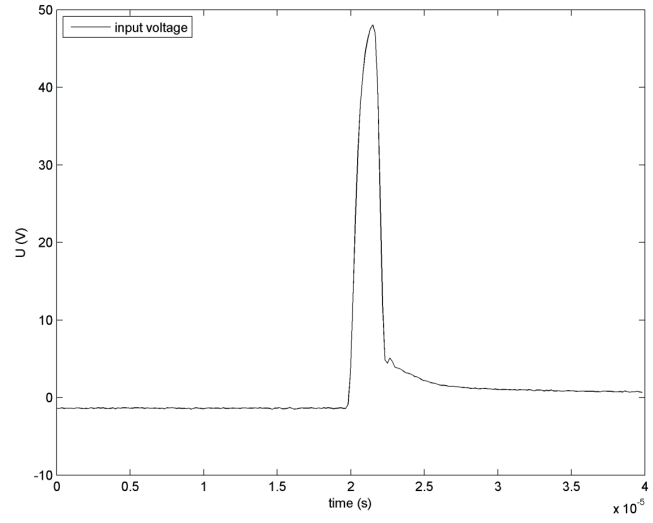

Figure 8. Measured excitation – chopped wave (CF)

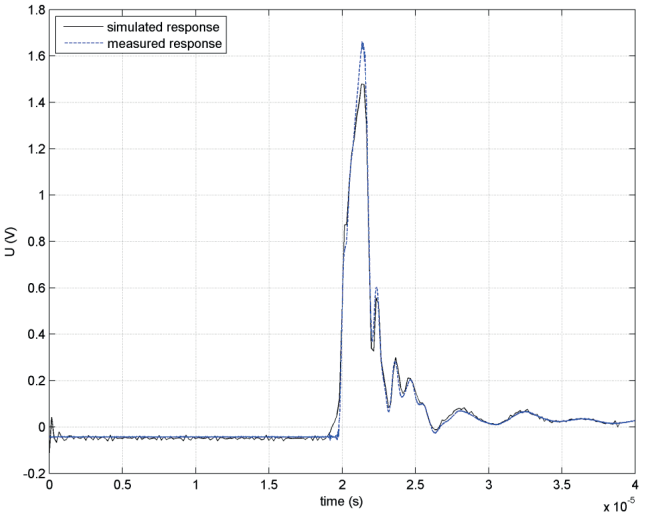

Figure 9. Comparison of measured and simulated response for the chopped wave excitation (CF)

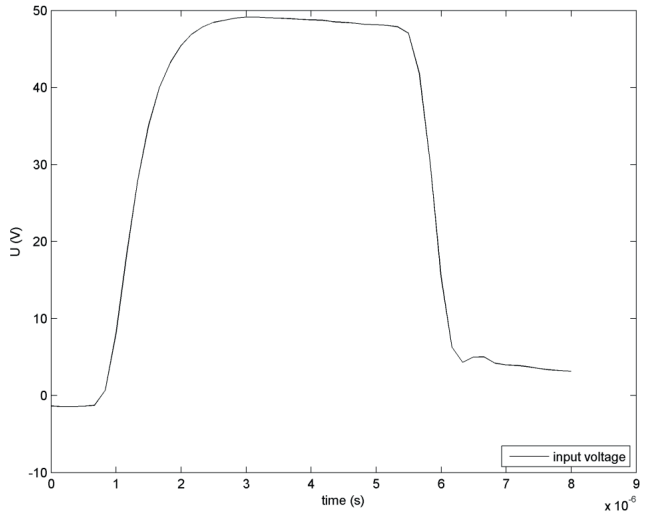

Fig. 10. Measured excitation – chopped wave (CT)

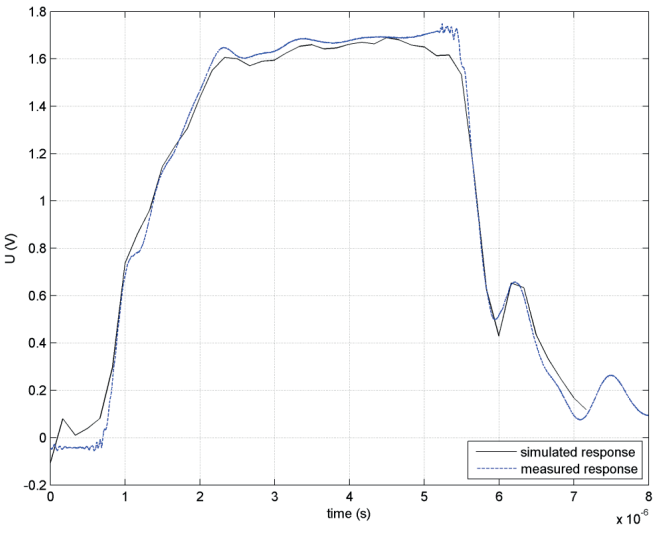

Fig. 11. Comparison of measured and simulated response for the chopped wave excitation (CT)

Lightning impulse chopped on the tail (LI-CT)

The third set of time-domain measurements was performed using the lightning impulse chopped on the tail according to IEC 60060-1, with chopping time of around 5 μs. All settings were the same as in (A), except the sample interval of the oscilloscope, which was 0.8 ns. Fig. 10 depicts the measured input voltage, while Fig. 11 gives the comparison of the simulated and measured response in the time-domain. The simulated time-domain response is shifted "in left" for 5 samples, to compensate the modeling delay.

FIlter Order Selection

With the increase of the filter order, a better fit of the model and the measurements is achieved. As the trade-off between complexity of the model and the better fit to the data, different order-selection criteria can be applied. Several order selection criteria [23-30] can be systemized as generalized information criterion (GIC). It can be approximated using the variance estimate

$$\hat{\sigma}^2 = \frac{1}{N}\|y - \hat{y}\|^2 \tag{16}$$

as

$$GIC = \text{constant} + N \ln \hat{\sigma}^2 + \nu m \tag{17}$$

where N denotes the number of samples in the data vector, m denotes the number of estimated parameters andis the penalty factor for the increase of the model size. The model order m is selected as the minimum of GIC for the proposed model orders between 0 and some maximum candidate. For finite values of N, the corrected Akaike criterion (AICc):

$$\nu = \frac{2N}{N - m - 1} \tag{18}$$

is suitable for the order-selection, with a smaller risk of overfitting compared to the Akaike criterion (AIC). AICc was already applied as the order-selection criteria in the impulse response modeling of the voltage instrument transformers [31].

The example of order-selection based on AICc is performed using model orders spanning from 1 to 1598, where the variance estimate (16) is calculated as the Euclidean distance between measured and calculated frequency response, for the frequencies determined by the data set of the measurement. Here, N is the number of frequency samples in the measurements. The adequate filter order according to AICc appeared to be L_{AICc}=71. Fig. 12 depicts the comparison of the simulated and measured response in the time-domain for the lightning impulse chopped on the tail (LI-CT). The simulated time-domain response is shifted "in left" for 5 samples, to compensate the modeling delay. The routine for calculation of AICc was programmed in MATLAB by the authors.

Figure 12. Comparison of measured and simulated response for the chopped wave

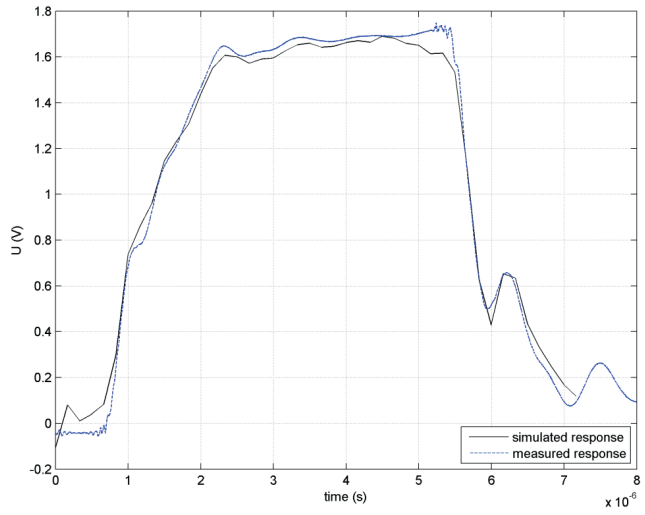

excitation (CT) – filter order is selected according to AICc

Conclusions

This paper describes a novel approach in the modeling of transformers, suitable for time-domain simulation of their response during the fast transients. On the basis of the frequency-domain measurements using a low-frequency network analyzer with the gain-phase test port, the z-domain, finite impulse response (FIR) model of the system function is built. The proposed technique is based on Wiener filtering and the frequency domain approach in the system identification. Since the proposed technique applies finite impulse response filtering, the z-domain model of the transformer is absolutely stable. Such a model, being a digital FIR filter, allows easy computation of the response of the system to various exciting voltages without a need for the measurements in the time-domain to be performed again for each transient excitation. Furthermore, Wiener modeling of the system function allows unequal spacing of the frequency samples. This gives the possibility of greater accuracy of the modeling in the frequency range where the magnitude or phase response of the system varies greatly. The linearity of the transformer is confirmed applying the Fourier analysis and different waveforms of the primary voltage, and methods for the model order selection, based on the generalized information criterion are discussed and applied. The theoretical analysis is confirmed with measurements in time domain, using the recurrent surge generator, and a very good matching is achieved between the simulated and measured time-domain responses for several different transient excitations.

Acknowledgment

This work has been fully supported by the Croatian Science Foundation under the project number IP-2013-1118.

References

[1] Q. Su, R.E. James, D. Sutanto, "A z-transform model of transformers for the study of electromagnetic transients in power systems," IEEE Transactions on Power Systems, vol. 5, no. 1, February 1990, pp. 27-32.

[2] Akcay, S. Islam, B. Ninnes, "Identification of power transformer models from frequency response data: A case study," Signal Processing, 68(1998), pp. 307-315.

[3] T. Noda, A. Ramirez, "z-Transform-Based Methods for Electromagnetic Transient Simulations," IEEE Transactions on Power Delivery, vol. 22, no. 3, 2007, pp. 1799-1805.

[4] B. Gustavsen, A. Portillo, R. Ronchi, A. Mjelve, "Measurements for validation of manufacturer's white-box transformer models," 4th International Colloquium "Transformer Research and Asset Management", Procedia Engineering 202 (2017), pp. 240-250.

[5] D. Filipović-Grčić, B. Filipović-Grčić, I. Uglešić, "High-Frequency Model of the Power Transformer Based on Frequency-Response Measurements," IEEE Transactions on Power Delivery, vol. 30, no. 1, February 2015, pp. 34-42.

[6] S.D. Stearns, R.A. David, Signal Processing Algorithms, Englewood Cliffs: Prentice Hall, 1988.

[7] B. Widrow, S.D. Stearns, Adaptive Signal Processing, Upper Saddle River: Prentice Hall, 1985.

[8] R.A. Horn, C.R. Johnson, Matrix Analysis, Cambridge: Cambridge University Press, 1990.

[9] J.E. Gentle, Numerical Linear Algebra for Applications in Statistics, Springer, 1998.

[10] S.D. Stearns, Digital Signal Processing with Examples in MATLAB, Boca Raton: CRC Press, 2003.

[11] G. C. Goodwin and K. S. Sin, Adaptive Filtering: Prediction and Control. Englewood Cliffs, NJ, USA: Prentice-Hall, 1984.

[12] P. A. Nelson and S. J. Elliott, Active Control of Sound. London, U.K.: Academic, 1992.

[13] Zentner, R.; Dadić, M.; Šipuš, Z.; Bartolić, J.: Time Domain Analysis of Mutual Coupling Measurements between Stacked Patches. ICECom 2003 Conference Proceedings / 17th International Conference on Applied Electromagnetics and Communications. Dubrovnik 2003, 370-373.

[14] Dadić M, Vasić D, Bilas V. A system identification approach to the modelling of pulsed eddy-current systems. NDT & E International 2005;38(2): 107-111.

[15] Martin Dadić, Petar Mostarac, and Roman Malarić, Wiener Filtering for Real-Time DSP Compensation of Current Transformers over a Wide

Frequency Range, IEEE Transactions on Instrumentation and Measurement, Vol. 66, No. 11, Nov. 2017, pp. 3023-3031.

[16] Keysight Technologies: Measuring Frequency Response with the Keysight E5061B LF-RF Network Analyzer, Application Note, http://literature.cdn-keysight.com/litweb/pdf/5990-5578EN.pdf (accessed September 18, 2018)

[17] Dadić, Martin; Petrović, Karlo; Malarić, Roman. FEM analysis and design of a voltage instrument transformer for digital sampling wattmeter: MIPRO 2017 Proceedings, Opatija : MIPRO, 2017. pp. 174-178.

[18] C. Wm. T. McLyman, Transformer and Inductor Design Handbook, 4th Edition, CRC Press, 2011.

[19] G. Koehler, "The Design of Transformers for Audio-Frequency Amplifiers with Preassigned Characteristics," Proceedings of the IRE, vol. 16, no. 12, pp. 1742-1770, 1928.

[20] T. Jelaković, Transformatori i prigušnice, Biblioteka časopisa „Elektrotehničar", Zagreb 1952.

[21] F. E. Terman, Radio Engineer's Handbook, McGraw, 1943.

[22] Arguimbau LB. *Vacuum-Tube Circuits and Transistors*. Wiley: New York, 1956.

[23] Stoica P, Selén Y. A review of information criterion rules. IEEE Signal Processing Magazine. vol. 21, no. 4, 2004, pp.36-47.

[24] Selén Y, Gudmundson E, Stoica P. An Approach to Sparse Model Selection and Averaging. IMTC 2006 – Instrumentation and Measurement Technology Conference. Sorento Italy 24-27 April 2006, pp.113-116.

[25] Broersen PMT. Finite Sample Criteria for Autoregressive Order Selection. IEEE Transactions on Signal Processing. Vol.48, no.12, 2000, pp.3550-3558.

[26] Tjärnström F, Ljung L. L_2 model reduction and variance reduction. Automatica, vol. 38, 2002, pp.1517-1530.

[27] de Waele S, Broersen P.M.T. Order Selection for Vector Autoregressive Models. IEEE Transactions on Signal Processing, vol. 51, no.2, 2003, pp. 427-433.

[28] Söderström T, Stoica P, Friedlander B. An indirect prediction error method for system identification. Automatica, vol.27, no.1, 1991, pp.183-188.

[29] Young P, Jakeman A, McMurtries R. An instrumental variable method for model order identification. Automatica, vol. 16, 1980, pp. 281-294.

[30] Djurić PM. Asymptotic MAP criteria for model selection. IEEE Transactions on Signal Processing, vol. 46, no. 10, 1998, pp.2726-2735.

[31] Dadić M, Keitoue S., Malarić R., Gazivoda S. FIR modeling of voltage instrument transformers with iron core for the study of fast transients, Measurement, vol. 43, no. 10, 2010, pp. 1404–1415